Iraqi Journal of Physics, 2020 *Vol.18, No.45, PP. 9-20*

DOI: 10.20723/ijp.18.45.9-20

Prospect of CW Raman laser in silicon- on- insulator nano-waveguides

Z. S. Khaleefa, Sh. S. Mahdi, S. Kh. Yaseen

Department of Physics, College of Science for Women, University of Baghdad, Iraq

E-mail: shaim@physik.tu-berlin.de, smsddzzz@yahoo.com

Corresponding author: zainabsalam6480@gmail.com

Abstract

Numerical analysis predicts that continuous-wave (CW) Raman lasing is possible in Silicon-On-insulator (SOI) nano-waveguides, despite of presence of free carrier absorption. The scope of this paper lies on lasers for communication systems around 1550 nm wavelength. Two types of waveguide structures Strip and Rib waveguides have been incorporated. The waveguide structures have designed to be 220 nm in height. Three different widths of (350, 450, 1000) nm were studied. The dependence of lasing of the SOI Raman laser on effective carrier lifetime was discussed, produced by two photon absorption. At telecommunication wavelength of 1550 nm, Raman lasing threshold was calculated to be 1.7 mW in Rib SOI waveguide with dimensions width (W= 450 nm) and Length (L= 25 mm). The obtained Raman lasing is the lowest reported value at relatively high reflectivities. Raman laser in SOI nano-waveguides presents the important step towards integrated on-chip optoelectronic devices.

Key words

Silicon (Si) photonics, Raman effect and photonic integrated circuits (P-ICs).

Article info.

Received: Dec. 2019
Accepted: Apr. 2020
Published: Jun. 2020

اقتراح ليزر رامان السيلكوني ذي الامواج المستمرة في موجه الموجه النانوي (السيلكون على عازل)

زينب سلام خليفة، شيماء صالح مهدي، سمير خضر ياسين

كلية العلوم للبنات، قسم الفيزياء، جامعة بغداد، العراق

الخلاصة

تتوقع نتائج محاكاه التحليل العددي أن ليزر رامان النانوي ذو الموجات المستمرة (CW) ممكن توليده في تراكيب أدلة موجه الموجات السيليكونية (SOI)، على الرغم من وجود امتصاص الحاملات الحره. الهدف من هذه الورقة يكمن على الليزرالمستخدم في انظمة الاتصالات حول الطول الموجي 1550 نانومتر. لقد تم اعتماد نوعين من هياكل موجه الموجي (Strip and Rib structures) في الدراسة.ايضا صممت تراكيب موجه الموجي لتكون 220 نانومتر في الارتفاع. اضافة الى ذلك تمت دراسة ثلاثة انواع مختلفة من العرض (350، 450، 1000) نانومتر. حيث نوقش اعتماد انتاج الليزر على عمر الحامل الفعال، الذي يتم توليده بواسطة عملية امتصاص فوتونين. عند الطول الموجي المستخدم في مجال الاتصالات 1550 نانومتر، تم حساب قدرة عتبة الليزر لتكون 1.7 ميجاوات في موجه الموجة Rib مع (عرض 450 نانومتر وطول 25 مم). حيث إن عتبة الليزر التي تم الحصول عليها من الدراسة هي أدنى قيمة في حالة قيم الانعكاسات عالية نسبيًا. بينت نتائج هذة المحاكاة، ان عتبة الليزر تقل كلما زادت قيمة الانعكاسات وقلت قيم الخسارة الناتجة من عملية الامتصاص الخطي والاخطي. ويعتبر ليزر رامان السيلكوني في دليل الموجات المتناهية الصغر الخطوة المهمة نحو الأجهزة الإلكترونية الضوئية المدمجة على الرقاقة، قد يفتح الطريق امام دارات ضوئية متكاملة.

Introduction

Silicon (Si) photonics is the new technology for the manufacture of optical devices and circuits using silicon as the core material for the integration of optical and electronic components with the standard manufacturing process of CMOS (complementary metal oxide semiconductor) [1]. The Si performs

well in the ranges of mid-wave, long-wave and very long-wave infrared (THz). It enables the integration of optical devices into silicon-on-insulator (SOI) wafers [2]that provide the route and manipulate the light. Integration of optoelectronic devices on SOI with CMOS technology enables low cost and large-scale production. Integrated Silicon optoelectronic devices have the potential to be miniaturized and mass-produced for many applications and markets, including telecommunications, optical interconnections, biological and chemical sensing [3]. To connect various components, the present computers use copper wires. These copper wires degrade the signal strength and have a maximum length limited. Researchers tried to substitute copper cables with optical technology. Instead of electrons, they used photons to carry out the information on computers. The future of the IC industry depends on speed and bandwidth, but have speed and bandwidth limitations in metallic interconnections. With the advancement of computer technology, we are now more dependent on ultra-fast information transfer rates between and within chips. By using optics, the data can flow at a higher speed when incorporating the optical components into a single silicon chip [1].

Silicon has a low efficiency to produce light emission through Radiative recombination process, because of its indirect bandgap semiconductor nature. Si with bandgap of (1.12) eV is transparent at wavelengths used typically for optical communication transmission from (1270– 1625) nm [1]. It has many of important properties which make it a good material, as wafers of silicon are incredibly pure, high thermal conductivity and large reflective index contributes the silicon as an excellent element for Raman crystal. Therefore it presents as an ideal platform for electronics and integrated optics focused on realizing active functionality, commonly light amplification, modulation and wavelength conversion in silicon waveguides. Numerous methods to induce light generation in silicon material have been proposed in the literature, such as SiGe quantum cascade structures [4], erbium-doped silicon nano-crystals [5], and surface-textured silicon bulk, where the texturing increases the photon emission [6]. Though, each of the previous approaches can create non-trivial limitations, making many research groups to explore the use of stimulated Raman scattering (SRS) in silicon as the main physical effect to get a medium gain. In actual fact, silicon as a transmission medium has much larger nonlinear effects than the generally used silicon dioxide, particularly the Raman Effect. The Raman gain has been successfully exploited in fiber amplifiers and lasers, but typically several kilometers of fiber are required to form a practical device.
The Raman amplification method used to amplify stokes wave via Raman interaction with the pump power. The Raman Scattering effect is inelastic scattering, when light beam propagates into an optical waveguide, the photons are scattered to new frequencies causing change in the energy of scattered photons. In this interaction, the energy may be losing or gains leading to Stokes shift or anti-Stokes shift, respectively. Stimulated Raman scattering (SRS) process in SOI is an attractive way of amplifying optical signal, because it does not require any dopants through fabrication of the SOI wafer and the amplified wavelength can be selected almost freely by using

pump light of an appropriate shifted wavelength [7].

Small cross sections, low loss waveguides and optimum waveguide lengths are required for the realization of high performance devices. Surface roughness produces strong scattering and high loss Because of the high index contrast between the core and the cladding [8], e.g. the losses of silicon tend to increase with reduction in dimension of cross-section. SOI waveguide fabrication processes via CMOS technology promise sub-micron cross section with low loss waveguides [9].

This paper is organized as follows. In section two, the simulation part of mode profile. In section three, the mathematical model to simulate and design a Raman laser based on the Raman Effect in the SOI waveguide. The proposed modeling includes the nonlinear interaction effects between the pump and Stokes signals in terms of SRS, two photon absorption (TPA), free carrier absorption (FCA), where the free carriers are generated mainly by the TPA of the pump. In section four, to find the threshold pump power, show numerical results CW laser simulations. Finally, section five summarizes the conclusions.

Several advances were produced in light emitters based on silicon and laser sources. Researchers initially concentrate on quantum dot lasers and the fusion of impurities into silicon like neodymium, but these efforts are not useful. Researchers subsequently operate on some other options [1]. The concept of using SRS in silicon waveguides was suggested in 2002 [9]. One year ago, the Jalali team demonstrated the first Raman Effect-based Si laser. But it has FCA and means carrier lifetime problems that make the gain in silicon waveguides difficult to achieve. FCA appears when a material absorbs a photon and a carrier is excited to an excited state (in the same band) from a ground state. In 2004, a lasing experiment involving silicon as a gain medium was reported using SRS where an 8-m-long optical fiber formed the ring laser cavity [10]. In 2005 [11], the Rong group published the first Si Raman laser continuous wave based on reversed biased p-i-n Si waveguide design. A pulsed pump power of 39 W with a pulse width of 3 picoseconds and a repetition rate of 25 MHz in SOI waveguides with a modal area of 2 μm^2 and a length of 25 mm was used to achieve the Silicon Raman laser [12]. Using a high-quality (high-Q) nanocavity design at the optically pumped sub microwatt threshold, a Raman silicon laser was achieved [13]. Here report the theoretical studied of Raman lasing in different dimensions, Raman lasing in SOI Nano-waveguides has been studied by numerically solved coupled equations, which describe the evaluation of the pump and Stokes wave via commercial software. Different dimensions of waveguide structures were reported in length (3, 6, 8, 10, 12, 16, 20, 25, 30, 35, 40, 45, 50, 60, 65, 70, 75, 80, 95, 95, 100, 110, 115) mm, width (350, 450, 1000) nm, and height compatible with the 220 nm CMOS method. Included are two kinds of Strip and Rib waveguides integrated. The inner core (in the order of hundreds of nanometers) is designed with a high refractive index silicone material surrounded by a low refractive index of silica cladding that provides high light containment. This study represents a significant step towards the production of practical continuous-wave optical lasers that can be incorporated into CMOS-compatible silicon chips with other optoelectronic parts.

Simulation part

Mode profiles were calculated using tool (FullWave) by R-software for all of our Strip and Rib waveguide buildings. To decrease the contamination effect, assume that our waveguide buildings are covered with a SiO_2 layer. In the calculation of the mode profile, refractive indices of 3.477 and 1.455 for Silicon and SiO_2 were adopted. The calculations demonstrate the possibility of coupling only the fundamental mode with a waveguide structure of 350 nm in width and coupling more than the fundamental mode with waveguide widths of 450, 1000 nm. The results of our simulation were shown in Figs. 1 and 2, showing only the fundamental mode. In the software calculated numbers, the efficient refractive indices are shown. For both Figs. 1 and 2, the right side indicates the profile of the computed mode. The left side indicates the waveguides of the Strip and Rib. The core waveguide's effective area is described as [14].

$$A_{eff}\frac{[\iint I(x,y)dxdy]^2}{\iint I^2(x,y)dxdy} \quad (1)$$

where I(x, y) is the transverse intensity of the fundamental mode (TE mode) of a waveguide (the integration is over the transversal plane). Considering only the calculation of the transverse mode profile for the fundamental mode, the effective core area could be estimated for each waveguide.

The effective core areas could be estimated for each waveguide, as shown in Fig.3 and Table 1. Assuming that only the fundamental mode coupled out of the waveguide at stokes signal, the full width value of the outcoupled mode profile at half peak (FWHM) can be determined from the vertical and horizontal cut mode profile. As shown in Fig.3.

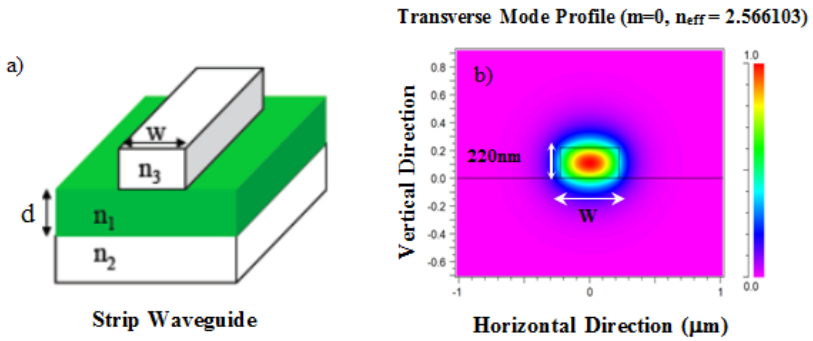

Fig.1: a) Basic block structure of Strip waveguide. b) Computed transverse mode profile of stokes signal in the SOI waveguide.

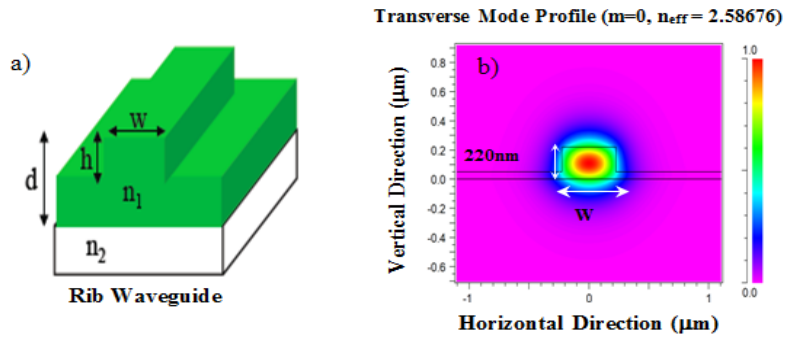

Fig.2: a) Basic structure of Rib waveguide. b) Computed transverse mode profile of stokes radiation in the SOI waveguide.

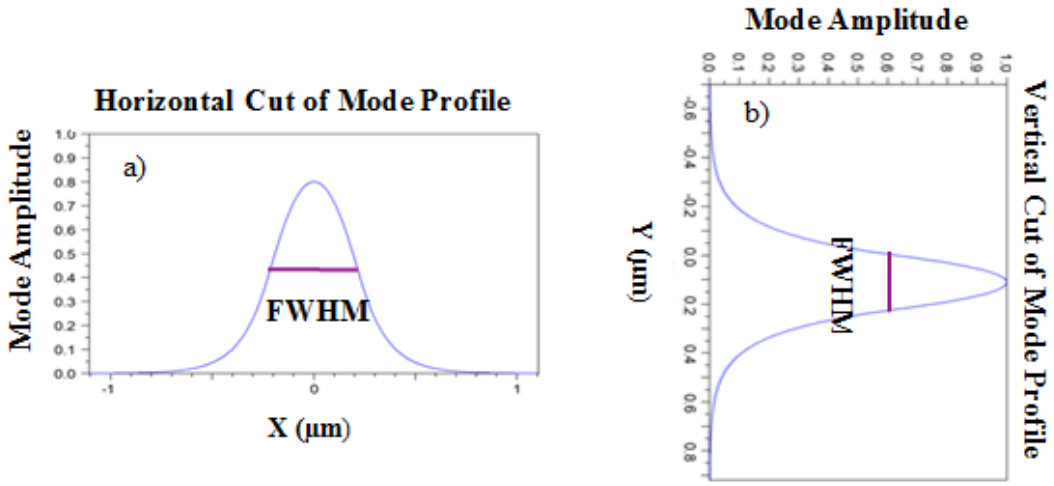

Fig.3: The computed transverse fundamental mode profile of stokes signal for rib waveguide width of 450 nm, a) horizontal cut and b) Vertical cut.

Table 1: The calculated effective area (A_{eff}), effective refractive indices (n_{eff}) of waveguides with 350, 450 and 1000 nm in width, 220 nm in height for Strip and Rib waveguide.

Rib/Strip (width Slab – height)	n_{eff} @ 1550nm	A_{eff} (μm^2) @ 1550nm
350 nm, 0 nm	2.102149	0.113977
450 nm, 0 nm	2.386479	0.126323
1000 nm, 0 nm	2.746367	0.244736
350 nm, 50 nm	2.276466	0.138204
450 nm, 50 nm	2.464671	0.112799
1000 nm,50 nm	2.7524445	0.252889

Mathematical model

A weak signal and a strong pump are launched into the optical waveguide, which leading to amplify the signal, due to the Stimulated Raman Scattering method. The distinction in energy between the pump and the signal (p, s) is called the vibration state ($\Omega = \upsilon_p - \upsilon_s$), which determines the frequency shift of the pump and Stokes ($\upsilon_{p,\ s}$) and shape of the Raman gain curve [15].

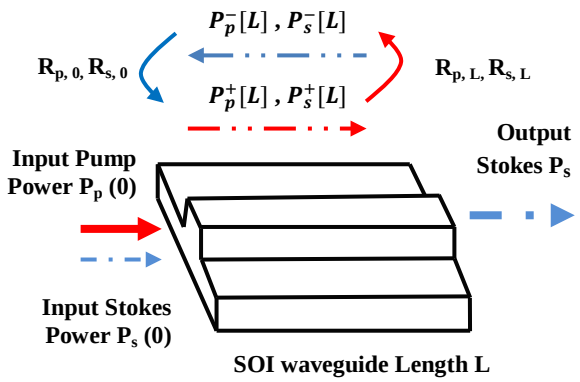

Fig.4: Schematic diagram of a basic silicon Raman laser.

Fig.4 displays the silicon Raman laser schematic diagram for a length L silicon waveguide, with Pp (0) being the started pump power. At Stokes wavelength, Raman scattering produces optical power. The pump power that propagates in the forward direction along the waveguide is expressed as $P_p^+[z]$, while $P_p^-[z]$, and expresses this process in the revers direction. The longitudinal evolution of the forward (+) and backward (-) propagating pump and Stokes powers $P_p^{\pm}[z]$ and $P_s^{\pm}[z]$. The first two boundary conditions are related to the forward and reverse propagating pump waves P $P_p^{\pm}$ on the waveguide end faces as well as the pump power P_0 injected as:

$$P_p^+[0] = T_0\, P_0 + R_{p,0}\, P_p^-[0],$$
$$P_p^-[L] = R_{p,l}\, P_p^+[L] \quad (2)$$

where (P_0) is the pump power, (T_p) is the silicon waveguide coupling efficiency. Where ($R_{P,\,0}$, $R_{P,\,L}$) for the input and output sides of the waveguide are the reflectivities at pump wavelengths, respectively.

The other two border conditions are related to the power of the forward and backward propagating Stokes waves $P_s^{\pm}$ at the waveguide end faces by the corresponding power reflectivities.

$$P_s^+[0] = R_{s,0}\, P_s^-[L]$$
$$P_s^-[L] = R_{s,l}\, P_s^+[L] \quad (3)$$

where ($R_{s,\,0}$, and $R_{s,\,L}$) are the waveguide input and end sides reflectivities at Stokes wavelengths, respectively. An optical cavity (optical feedback) can be used to increase circulation within the silicon waveguide. To describe the impact of cavity enhancement on nonlinear optical interaction, a theoretical model was taken as follows:

$$\pm\frac{1}{P_p^{\pm}}\frac{dP_p^{\pm}}{dz} = -\alpha_{lin} - \alpha_{non-lin}^{FCA}(z) - \frac{g}{A_{eff}}\frac{\lambda_s}{\lambda_p}\left(P_s^{\pm}(z) + P_s^{\mp}(z)\right) - \frac{B}{A_{eff}}(P_p^{\pm} + 2P_p^{\mp} + P_s^{+} + P_s^{-}) \quad (4)$$

$$\pm\frac{1}{P_s^{\pm}}\frac{dP_s^{\pm}}{dz} = -\alpha_{Lin} - \alpha_{non-lin}^{FCA}(z) - \frac{g}{A_{eff}}\left(P_p^{\pm}(z) + P_p^{\mp}(z)\right) - \frac{B}{A_{eff}}(P_s^{\pm} + 2P_s^{\mp} + P_p^{+} + P_p^{-}) \quad (5)$$

$$\alpha_{non-lin}^{FCA}(z) = 1.45 * 10^{-17}\left(\frac{1.45}{1.55}\right)^2 * N_{eff} \quad (6)$$

$$N_{eff} = B * \{(P_p^+)^2 + \left(P_p^-\right)^2 + (P_s^+)^2 + (P_s^-)^2 + 4\left(P_p^+P_p^- + P_s^+P_s^- + P_p^+ + P_p^- + P_p^+ + P_p^-\right\} * \frac{(\tau_{eff})}{2h\nu_p * {A_{eff}}^2} \quad (7)$$

At threshold pump P_0, the Stokes powers $P_s^{\pm}$ are much smaller than the pump powers $P_p^{\pm}$, therefore Eqs. (4-7) can be written as:

$$\pm\frac{1}{P_p^{\pm}}\frac{dP_p^{\pm}}{dz} = -\alpha_{lin} - \alpha_{non-lin}^{FCA}(z) - \frac{g}{A_{eff}}\frac{\lambda_s}{\lambda_p}\left(P_s^{\pm}(z) + 2P_s^{\mp}(z)\right) \quad (8)$$

$$\pm\frac{1}{P_s^{\pm}}\frac{dP_s^{\pm}}{dz} = -\alpha_{Lin} - \alpha_{non-lin}^{FCA}(z) - \frac{g}{A_{eff}}\left(P_p^{\pm}(z) + 2P_p^{\mp}(z)\right) \quad (9)$$

$$\alpha_{non-lin}^{FCA}(z) = 1.45 * 10^{-17}\left(\frac{1.45}{1.55}\right)^2 * N_{eff} \quad (10)$$

$$N_{eff} = B * \{(P_p^+)^2 + \left(P_p^-\right)^2 + 4P_p^+P_p^-\} * \frac{(\tau_{eff})}{2h\nu_p * {A_{eff}}^2} \quad (11)$$

where (g) is the effective Raman gain constant. (α_{lin}, $\alpha_{non-lin}^{FCA}$) are defined as the linear absorption coefficient (see Table 2) and nonlinear absorption coefficient contribution to the free carrier generation at pump/Stokes wavelengths, respectively. And (N_{eff}) is the density of free charge carrier.

Table 2: In Silicon nano-waveguides, Linear loss ($\alpha_{p,s}$).

linear losses of $\alpha_{p,s}$ (dB/cm)	**Reference**
0.5	[16]
1	[14, 17]
2.8	[18]
3.6	[19, 20]
4	estimate
5	estimate

The laser is at the threshold when the Stokes round trip net gain is equal to the losses due to the wave guide's reflectivity ($R_{s,0}$ and $R_{s,L}$) outcoupling on the left and right end faces. y numerical solving Eqs. (9), (11) and (3), thus obtain the oscillation condition of the laser threshold as:

$$R_{s,0}\,R_{s,L}\,\mathrm{Exp}[2\int_0^L\left(-\alpha_{Lin}-\alpha_{non-lin}^{FCA}(z)-\frac{g-2B}{A_{eff}}\left(P_p^+(z)+2P_p^-(z)\right)\right)dz]=1 \qquad (12)$$

Simulation parameters

Focus initially on non-coated silicon waveguide lasers and conclude that all reflectivity is due to the silicon / air interface, $R_{p,0} = R_{p,L} = R_{s,0} = R_{s,L}$ = 30%. TPA coefficients $B_{p,s}$ = 0.5 cm/GW[21], the pump and Stokes wavelengths of λ_p = 1450nm and λ_p = 1550 nm, respectively. Our simulations are based on the design of the Strip and Rib waveguide, for which the different effective SRS areas are shown in Table 1.

Results and discussion

The longitudinal distribution of the energy of the pump is calculated numerically to find the laser threshold power P_{th}. Numerically solved Eq.(8) with the limit conditions in Eq.(2) and (11), taking into account both the forward and backward power on the pump waves. The laser threshold (P_0) can be calculated numerically by varying the pump power (P_0) until the Eq.(12) condition hasbeen fulfilled. As shown in Fig.5, the estimated pump power threshold for starting Raman lasing was calculated from Eq.(12) as a function of SOI waveguide length at different linear losses, see Table 2.

The results indicate that a silicon Raman laser (all our structures) should be able to be pumped beyond the threshold using a pump with just a few miliwatts of output power. It is clear that there is a very small increase in the laser threshold in the waveguide length range from (100 to 115) mm at a linear loss of 0.1cm^{-1} and a small increase in the laser threshold in the from (40 to 50) mm at a loss of range 0.2 cm^{-1}, for all types of Strip and Rib waveguides. Lengthening the waveguide above (45 to 115) mm will result in a significant rise in the lasing threshold at a loss of 0.2 cm^{-1}. But in the range of (6 to 30) mm of a waveguide length, there is a sharp rise in the lasing threshold at other values of loss. Because of influence cavity losses, the necessary threshold pump powers are increased. Also, outside the following ranges, there is a limited usable range of waveguide lengths; the waveguide will never start lasing. For example, Waveguide with a linear loss of 0.7 cm^{-1} does not have a laser threshold at lengths of (30-115) mm in our calculated results. Also, if a linear loss is (0.9-1) cm^{-1}, there is no lasting limit at lengths of (20-115) mm. A linear loss of (1.25) cm^{-1} does not

predict a lasting threshold of (16-115) mm in length. Fig.5 shows that the threshold power of the pump is increased by increasing the linear loss. In Fig.5, the structures of the Strip SOI obtained a minimum threshold pump power of approximately 9.5 mW for L=(50, 55, 60, 65) mm and W= 350 nm at a loss of 0.1cm^{-1}. While for the Rib waveguide W= 450nm, the minimum threshold input pump power of about 9.4mW at L= (50, 55, 60, 65) mm and Loss 0.1 cm-1 was achieved.

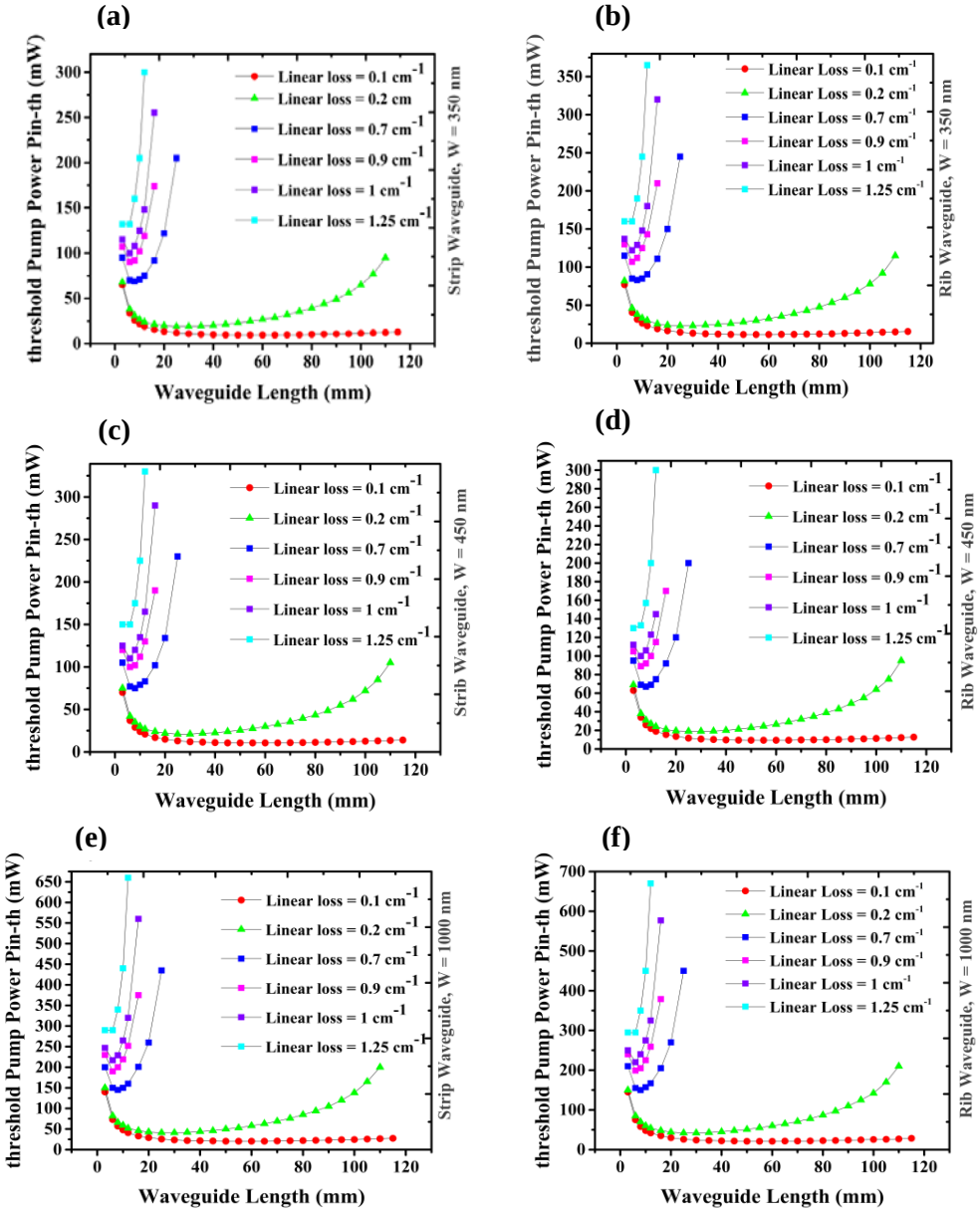

Fig.5: Threshold power of the silicon Raman lasers as a function of the various waveguide lengths at a different waveguide linear loss. End-face reflectivities ($R_{p,0} = R_{p,L} = R_{s,0} = R_{s,L}$) are 30%, and free-carrier absorption is assumed of (τ_{eff} = 0.1 ns). For a), c), e) Strip and b), d), f) Rib waveguides.

The impact of FCA can be much more intense, as demonstrated in Fig.6, as opposed to the minor impact of TPA. The estimated pump energy threshold for starting Raman lasing was calculated using the estimated reflectivities (30 %) from Eq.(12) for an effective free carrier life as a function of the different SOI waveguide lengths.

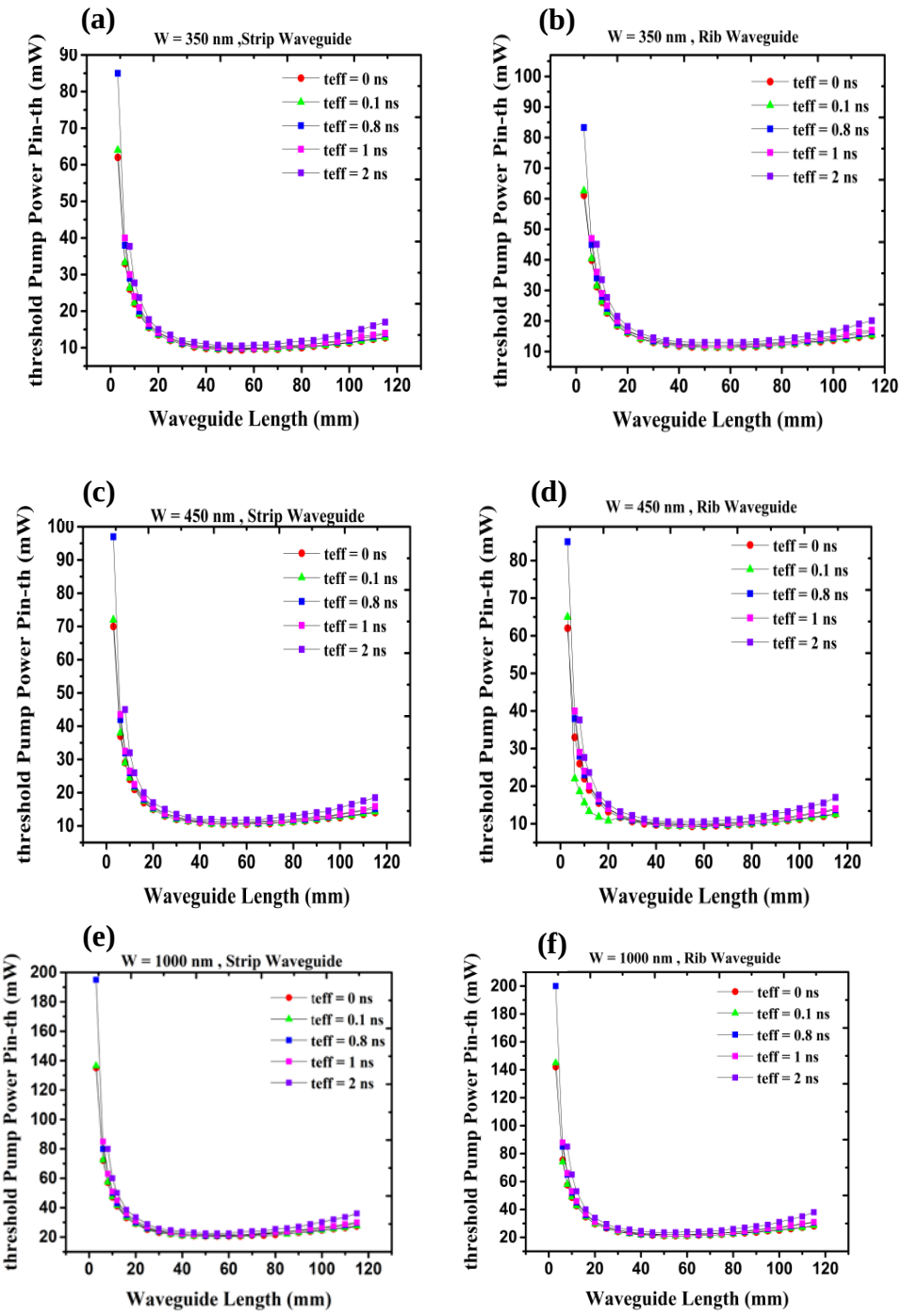

Fig.6: Threshold pump power of silicon Raman lasers as a function of the different waveguide lengths L for several effective carrier lifetimes (τ_{eff}) and α_p = α_s = 1 dB/cm. For a), c), e) Strip and b), d), f) Rib waveguides.

It is clearly shown in Fig.6 that minimum threshold CW power is limited by nonlinear loss. The effective carrier lifetime (τ_{eff}) plays an important role in the low pump power threshold into the silicon waveguide structures. Shorter carrier lifetime results in smaller carrier density. As shown in the calculation results, the output power becomes saturated at input pump power exceeding 1000nm. The effective carrier lifetime in Fig.6 are reported by various research groups (see Table 3).

Table 3: Effective charge (Carrier) lifetime in Si nano-waveguide.

Carrier Lifetime (ns)	Reference
0.1	[14]
0.8	[22]
2	[22]
6.8	[8]
10	[23]
25	[24]

It is obvious that the carrier lifetime decreases at smaller silicon waveguides size. This is due to the change in mechanisms of the recombination rate and smaller diffusion time; it is promising to have low threshold in submicron waveguide dimensions because of the shorter effective carrier lifetime (τ_{eff}) [13], [15]. At Strip 350 nm waveguide width, minimum threshold pump power of about 9.4 mW was obtained for different L= (50, 55) mm, and τ_{eff}= 0ns. While for the Rib waveguide of W = 450 nm, input pump power low threshold of about 9.3 mW was obtained at L=3 mm and τ_{eff} = 0ns. The effective free carrier lifetime is allowed to increase after which there will be no laser threshold. There is also a decrease in the usable scale of waveguide lengths as (τ_{eff}) rises. Outside this range e.g. for L = 3 mm at the range of τ_{eff} = (1-2) ns and for a range of τ_{eff} = 2 ns at rang of (3-10) and (105-115) mm, the device has no lasting threshold value.

In the final assumptions, we consider the left hand and right hand Stokes reflectivity of 90 % and the reflectivity of the left and right hand pumps of 0 % and 100 % respectively, see Fig.7.

Fig.7 shows the calculated threshold pump power of the high-reflectivity Raman laser against the waveguide length of a Strip and Rib waveguides for various effective carrier lifetimes. The ^{thresholds} are significantly smaller than in the first laser (see Fig.6), for a widths of (350, 450 and 1000) nm with a fixed linear loss of 0.1 cm^{-1}. At Strip SOI structures, minimum threshold pump power of about 1.8 mW was obtained for different L= (25-40) mm and W= 350 nm. While the input pump power low threshold of about 1.7 mW at all τ_{eff} values and L= (25, 30) mm was accomplished for the waveguide of W = 450 nm.

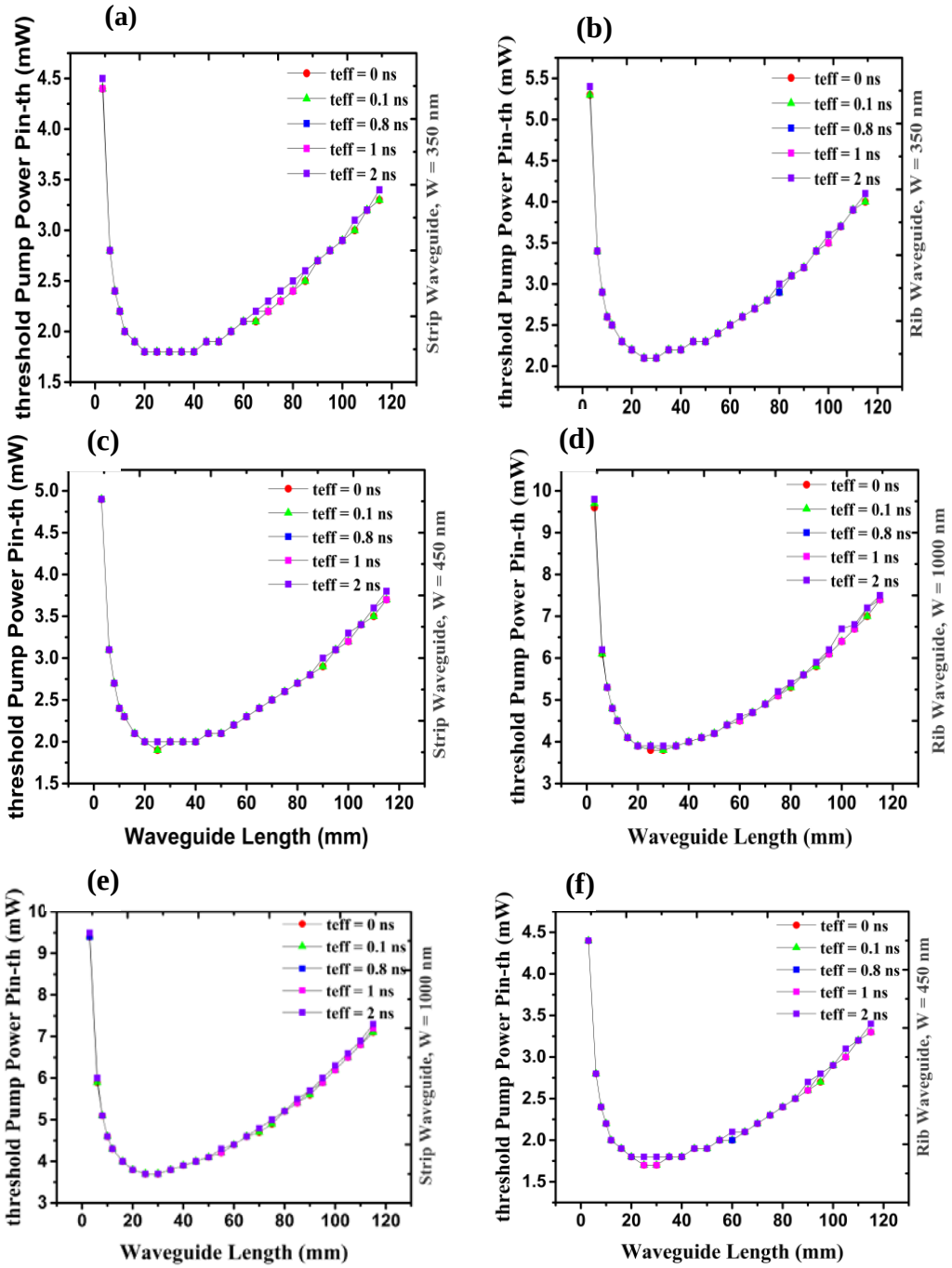

Fig.7: Threshold pump power versus waveguide length (L) for several effective carrier lifetimes. The Stokes reflectivities of 90% in both side, and left-hand and right-hand pump reflectivities of 0% and 100%, respectively.

The equivalent in laser threshold values between strip and rib waveguides is due to the agreement of the effective area values where the distributions of the mode are nearly the same. Our results suggest that high reflection leads to the conclusion that achieving low threshold power is not restricted in lengths or τ_{eff}.

Conclusions

Shown numerically that Raman lasing is possible in SOI waveguides with pump power laser on the order of a miliwatts, despite of presence of the effects of tow photon absorption and free-carrier absorption. Two different waveguide structures (Strip and Rib) were simulated. Low threshold power

was calculated to be 1.7 mW in rib SOI waveguide of 450 nm in width. The lowe pump threshold is the lowest reported value at relatively high reflectivities.450 nm of rib waveguide presents as an optimum width reaching low threshold power for Raman lasing, while 350 and 1000 nm is the optimum width for strip waveguide. Silicon photonics technology is an important step towards integrated on-chip optoelectronic devices. Further development, silicon photonics components and circuits on SOI platform for example, ring resonator, photonic crystal.

References

[1]A. Dhiman, IOSR J. Appl. Phys., 3 (2013) 67-79.
[2] R. Soref, IEEE J. Sel. Top. Quantum Electron, 12 (2006) 1678-1687.
[3] P. Cheben, R. Soref, D. Lockwood, G. Reed, Adv. Opt. Technol., 2008 (2008) 1-2.
[4] D.J. Lockwood, L. Pavesi, "Silicon Photonics", Springer New York, 2004.
[5] N. Daldosso, D. Navarro-Urrios, M. Melchiorri, L. Pavesi, C. Sada, F. Gourbilleau, R. Rizk, Appl. Phys. Lett., 88 (2006) 161901.
[6] K. Yamamoto, IEEE Trans. Electron Devices, 46 (1999) 2041-2047.
[7] M. Krause, "Efficient Raman amplifiers and lasers in optical fibers and silicon waveguides: new concepts", Ph.D. Thesis, Technische Universität Hamburg, (2007).
[8] A. Liu, H. Rong, R. Jones, O. Cohen, D. Hak, M. Paniccia, J. Light. Technol., 24 (2006) 1440-1455.
[9] B. Jalali, V. Raghunathan, D. Dimitropoulos, O. Boyraz, IEEE J. Sel. Top. Quantum Electron. 12 (2006) 412-421.
[10] O. Boyraz, B. Jalali, Opt. Express, 12 (2004) 5269-5273.
[11] R. Jones, H. Rong, A. Liu, A.W. Fang, M.J. Paniccia, D. Hak, O. Cohen, Opt. Express, 13 (2005) 519-525.
[12] V. Raghunathan, O. Boyraz, B. Jalali, Conference on Lasers and Electro-Optics (Optical Society of America), (2005) CMU1.
[13] D. Yamashita, Y. Takahashi, J. Kurihara, T. Asano, S. Noda, Phys. Rev. Appl., 10, 2 (2018) 24039-1_24039-15.
[14] M. Krause, H. Renner, E. Brinkmeyer, Opt. Express, 12 (2004) 5703-5710.
[15] V.R. Kumbhare, Int. J. Comput. Appl., 975 (2015) 8887.
[16] A.G. Rickman, G.T. Reed, IEE Proceedings - Optoelectronics, 141 (1994) 391-393.
[17] R. Claps, V. Raghunathan, D. Dimitropoulos, B. Jalali, Opt. Express, 12 (2004) 2774-2780.
[18] R. Claps, D. Dimitropoulos, Y. Han, B. Jalali, Opt. Express, 10 (2002) 1305-1313.
[19] R.L. Espinola, J.I. Dadap, R.M. Osgood, S.J. McNab, Y.A. Vlasov, Opt. Express. 12 (2004) 3713-3718.
[20] J.I. Dadap, R.L. Espinola, R.M. Osgood, S.J. McNab, Y.A. Vlasov, Opt. Lett., 29 (2004) 2755-2757.
[21] H. Rong, A. Liu, R. Nicolaescu, M. Paniccia, O. Cohen, D. Hak, Appl. Phys. Lett., 85 (2004) 2196-2198.
[22] T.-K. Liang, L.-R. Nunes, H.-K. Tsang, M. Tsuchiya, IEICE Electron. Express, 2 (2005) 440-445.
[23] H. Rong, A. Liu, R. Jones, O. Cohen, D. Hak, R. Nicolaescu, A. Fang, M. Paniccia, Nature, 433 (2005) 292-294.
[24] A. Liu, H. Rong, M. Paniccia, O. Cohen, D. Hak, Opt. Express, 12 (2004) 4261-4268.